

A novel electrostatic based microgripper (cellgripper) integrated with contact sensor and equipped with vibrating system to release particles actively

Hamed Demaghsi · Hadi Mirzajani ·
Habib Badri Ghavifekr

Received: 28 June 2013 / Accepted: 21 November 2013 / Published online: 3 December 2013
© Springer-Verlag Berlin Heidelberg 2013

Abstract This paper presents design and simulation of a novel electrostatic microelectromechanical systems gripper with an integrated capacitive contact sensor. Moreover, this microgripper is able to employ vibration to release micro objects (cells) actively. Lateral comb drive system is used to close the gap between the gripper arms and hold the objects while the transverse comb differential capacitances act as a contact sensor to prevent damaging the fragile micron-sized particles specifically biological cells. In addition, the capability of the microgripper in generating vibration at the end-effectors electrostatically is an advantage to facilitate releasing process by overbalancing the adhesion forces between the particle and the gripper arm. Finite element analysis based simulations are carried out to estimate the behavior of the microgripper while the standard SOI-MUMPs micromachining process is proposed for fabrication of the microgripper.

1 Introduction

The manipulation of micron-sized objects finds applications in many areas from assembly of MEMS and microelectronic devices to handling the bio-particles such as cells and bacteria. High precision, robustness and reliability with dimensions on the size-scale of the manipulated objects are

characteristics that enable MEMS-based microgrippers to be employed in micromanipulation specifically bio-micro-manipulation for handling flexible and fragile biological objects.

In the past two decades, various microgrippers have been developed for different applications which generally can be classified on the base of actuation system, sensing system and releasing strategy. Shape memory alloy (SMA), piezoelectric, electrothermal and electrostatic actuation systems are frequently used mechanisms that are employed for grasping the micro objects. In addition, for sensing, we can cite piezoresistive, piezoelectric, magnetic, capacitive and optical mechanisms (Pettrin 2009) which are able to measure end-effectors displacement or/and exerted force to micro particles.

SMA based microgrippers are made of shape memory alloys like NiTi which is based on a unique capability of reversible plastic deformation. This capability allows the alloys to have a permanent shape under a defined critical temperature, after warming-up they change their shape, but after cooling they return to their primary shape (Varona et al. 2009). High accuracy in micropositioning, large deflection and high recovery force (Millet et al. 2004) are of important advantages and having relatively big reaction time, large size, high working temperature and high power consumption (Varona et al. 2009) are some disadvantages of the SMA alloys. Kohl et al. (2002) designed a monolithic SMA gripper integrated with an optical positioning sensor. Kyung et al. (2008) fabricated a microgripper with flexible hinge structures actuated by SMA wires and equipped with strain gauge to control the gripping force.

The main feature of the piezoelectric materials is their ability to convert mechanical energy to electric energy and vice versa. It means by applying voltage on piezoelectric crystal it is deformed whereas by transmitting mechanical

H. Demaghsi (✉) · H. Mirzajani · H. B. Ghavifekr
Faculty of Electrical Engineering, Sahand University
of Technology, Sahand Town, Tabriz, Iran
e-mail: h_demaghsi@sut.ac.ir

H. Mirzajani
e-mail: h_Mirzajani@sut.ac.ir

H. B. Ghavifekr
e-mail: badri@sut.ac.ir

energy to this crystal, potential difference appears due to electrical polarization. Although piezoelectric microgrippers have fast response, generate relatively big force and are accurate in micropositioning (Millet et al. 2004), they require high operating voltage and are able to move just in small movement Goldfarb and Celanovic (1999). Raghavendra et al. (2010) reported a novel two-dimensional, compliant, monolithic piezo-actuated microgripper using flexure hinges and investigated the hinge parameters to achieve optimal performance of the gripper. Goldfarb and Celanovic (1999) designed a flexure-based microgripper actuated by piezoelectric ceramic and integrated with strain gauge to measure gripping force and displacement for precise positioning small-size particles.

Generally, thermal expansion of the structure due to joule heating effect is the basic principal of the thermal microactuators. Some advantages of this kind of actuator are: relatively large displacement, low operating voltage, high gripping force. However, generated extremely high temperature during operation limits its application in some research areas (Varona et al. 2009). Stavrov et al. (2010) designed a silicon-based normally closed microgripper equipped with piezoresistors to sense the gripper arms deflection. An electroplated nickel microgripper which operated by electrothermal bent beam (chevron) actuator was introduced by Kim et al. (2004). In this design, the metallic gripper was embedded in thick SU-8 adaptor as a mechanical supporter to make the handling operation easily. While most of the normally open microgrippers can only close the gap between the arms to hold the objects, Volland et al. (2007) fabricated a normally open gripper integrated with two thermal actuators that could both open and close the gap for increasing the gripping range.

Thermal polymeric microgrippers are great offer as a respond to growing demands for bio-micromanipulation. Unique characteristics of the polymers (e.g. SU-8 as a mostly-used polymer in the microgrippers) such as: structural rigidity, chemical resistance, biocompatibility, the ability to define high aspect ratio structures, electrically non-conductivity and most importantly large coefficient of thermal expansion (Chronis and Lee 2005) enable them to operate at low temperature and voltage. Thus, this kind of microgripper can be easily utilized in an ionic environment and physiological solutions to single cell manipulation and positioning, cell isolation, etc. (Chronis and Lee 2005). Chronis and Lee (2005) designed a microgripper based on U-shaped bent beam electrothermal actuator (heatuator) fabricated by SU-8 as the structural material and thin Cr/Au layer as a heater element. A novel microgripper based on silicon-polymer materials integrated with piezoresistive sensors was reported by Duc et al. (2008). Taking advantage of the high heat conductivity of silicon as well as high thermal expansion coefficient of SU-8, the

microgripper operated at the driving voltage of 4.5 V where the maximum temperature was 177 °C. While most of the researchers use piezoresistors as deflection/force sensor in the thermally actuated microgrippers, Mackay et al. (2013) designed a metallic-polymeric microgripper incorporated with a small silicon micro-mirror to estimate the tensile load applied to the gripped specimen.

Electrostatically-driven microgrippers' main advantages are temperature independence, no hysteresis, satisfactory amount of force generation, high frequency response (up to hundreds of kHz under resonance) and the lowest power consumption (Bazaz et al. (2011); Varona et al. 2009). However, relatively large operating voltage makes it incompatible with typical CMOS electronic drivers (Varona et al. 2009). Since most living objects such as cell and bacteria cannot sustain temperature and large force that are typical for thermally actuated grippers, electrostatic microgrippers are of great interest in bio-micromanipulation (Beyeler et al. 2007). Varona et al. (2009) designed a surface micromachined microgripper actuated by parallel-plate electrostatic mechanism. This gripper had a low operation range due to pull-in effect which limited the range of actuation in these kinds of grippers. Consequently, comb-drive systems which have stable drive over relatively long distance as well as linear electromechanical transfer functions for large displacements are used mostly in designing of the electrostatically-actuated grippers (Kim et al. 1992; Tang et al. 1989). Volland et al. (2002) fabricated a microgripper based on comb-drive systems which was able to deflect each gripper arm 20 μm at the operation voltage of 80 V. This gripper did not have sensing mechanism. Chen et al. (2010a, b) incorporated the vacuum tool into the electrostatic microgripper to use pressure for gripping and releasing the objects. The comb drives operated at 85 V to deflect the end-effectors 25 μm for holding the target. Bazaz et al. (2011) modeled and fabricated an electrostatic microgripper in which a lateral comb-drive system acted as the actuation part and a transverse comb differential capacitive sensor acted as the contact sensor to sense contact between micro-object and microgripper's jaws. Beyeler et al. (2007) reported a novel microgripper integrated with force sensor. In this design, one gripper arm was attached to the comb-drive system and the other arm was connected to the differential capacitive sensor; by applying voltage on comb-drives the micro-object is pushed by one jaw over the other one to activate the sensing part. Therefore this microgripper was able to estimate the gripping force. Chen et al. (2009) fabricated a microgripper in which both arms were attached to separate comb-drive systems that enabled it to move end-effectors independently. In this work, Chen et al. (2009) mostly focused on investigating the surface forces at micro scale dimensions and designing a plunger system to overcome these forces.

Since the handling objects are in the range of micrometer and nanometer, interactive forces such as van der Waals force, surface tension force and electrostatic force between micro/nano particles and gripper surface become more dominant (Arai et al. 1996). As a result, it is easy to pick up an object using the adhesion forces but the release process is very difficult (Fang and Tan 2006). To release objects rapidly and facilely, several strategies have been proposed in the past decade. Arai et al. (1996) analyzed the balance of the adhesion forces between the objects and proposed methods to reduce the adhesion forces based on the micro physics and also fabricated a gripper arm with rough surface to overcome the adhesion.

Generally there are two techniques for releasing process: passive release technique and active release technique (Chen et al. 2009). Passive release method depends on the adhesion forces between the micro object and substrate to detach the object from end-effector (Chen et al. 2009, 2010a, b). As an instance, Fuchiwaki et al. (2008) reported a piezoelectric–electromagnetic micromanipulator where ultraviolet cure adhesive was applied on the substrate to enable release. As a result, disadvantages such as: dependence on surface properties, being time consuming and being poor in repeatability cause that active release method is employed as a major strategy (Chen et al. 2009).

Active release method is independent of the substrate. In this case, by employing a system into microgripper object detaches from end effector. Park and moon (2005) reported a novel three-tungsten-based microgripper actuated with piezoelectric. The third auxiliary end-effector not only helped to grip the object securely but also facilitated releasing process by reducing the electrostatic forces between the object and chopsticks. Chen et al. (2009) designed a novel electrostatic microgripper which was integrated with a plunging system. That system was employed to impact micro objects for gaining sufficient momentum in order to overcome the adhesion force.

Vibration is a strategy to release an object. In fact, vibrating the end-effector generates enough inertial force to overbalance the adhesion forces (Fang and Tan 2006). Sinan Haliyo et al. (2003) fabricated a gold coated piezoresistive silicon micro beam to pick the micro object and employed vibration to overbalance adhesion to achieve the release. Chen et al. (2010a, b) fabricated a micro manipulation system including a MEMS-based microgripper fixed on a PZT ceramic. The electrostatic microgripper with piezoresistive force sensor was able to pick the micro object and vibrate the end-effectors horizontally (in-planely) and PZT vibrated the microgripper vertically. So the compound vibration takes the advantage of inertial effects to overcome the adhesion forces. In the previous work,

Demaghsi et al. (2013) used this idea and proposed a novel metallic (nickel) microgripper integrated with

electrostatically driven comb-drive systems to generate vibration at the end effectors in-planely to overbalance adhesion forces between nano particles and gripper's arm. It is worth noting that the electrothermal chevron actuator was employed to grip and transfer the objects and there was no sensing mechanism in this microgripper.

In according to above mentioned samples, some researchers just focus on the sensing part of the gripper without having any idea for releasing micro particles in an active method (Bazaz et al. (2011); Beyeler et al. 2007), on the other hand, Sinan Haliyo et al. (2003) and Chen et al. (2010a, b) utilized inertial effect as the active strategy for releasing objects but their microgrippers' force sensors were on the base of piezoresistive material which are complex in fabrication and low sensitive (Petrin 2009).

In this paper, we present a monolithically fabricated microgripper with the main features;

- (1) Electrostatic comb-drive actuation system which works at 55 V DC as the operation voltage while the end effectors are grounded to grasp the living cells safely.
- (2) Integration with capacitive contact sensor to protect the cells.
- (3) Specific comb drives to generate vibration electrostatically as the strategy for releasing the particle actively.

2 System configuration and design consideration

To use vibration as the active release method, we are going to deploy an electrical signal to vibrate the gripper in-planely. The frequency of the signal is the resonant frequency in which the gripper vibrates in-planely. This resonant frequency can be easily found by FEA-based simulation. Generally, the capacitors thickness in the capacitive sensing part is thinner than combs attached to the actuation shuttle and therefore vibrating the gripper at the desired resonant frequency causes the capacitors deflect undesirably. This kind of deflections makes poor functionality and even damage the gripper at the release phase. Unless, the capacitors are fabricated much thicker that cause more parasitic capacitance (Bazaz et al. 2011) and occupy more space.

As a result, because of the reasons; (1) No need to contact capacitive sensor at release phase and (2) avoid capacitor deflection due to vibration, we separate the actuation part and capacitive sensing part through a 2- μm gap. Therefore, to take the advantage of the vibration at the release phase, the electrical signals at the desired resonant frequency are employed to specific sets of comb drives which cause vibration at the actuation part and the end-effectors without any effect on sensing section.

Fig. 1 Schematic and detail view of the microgripper

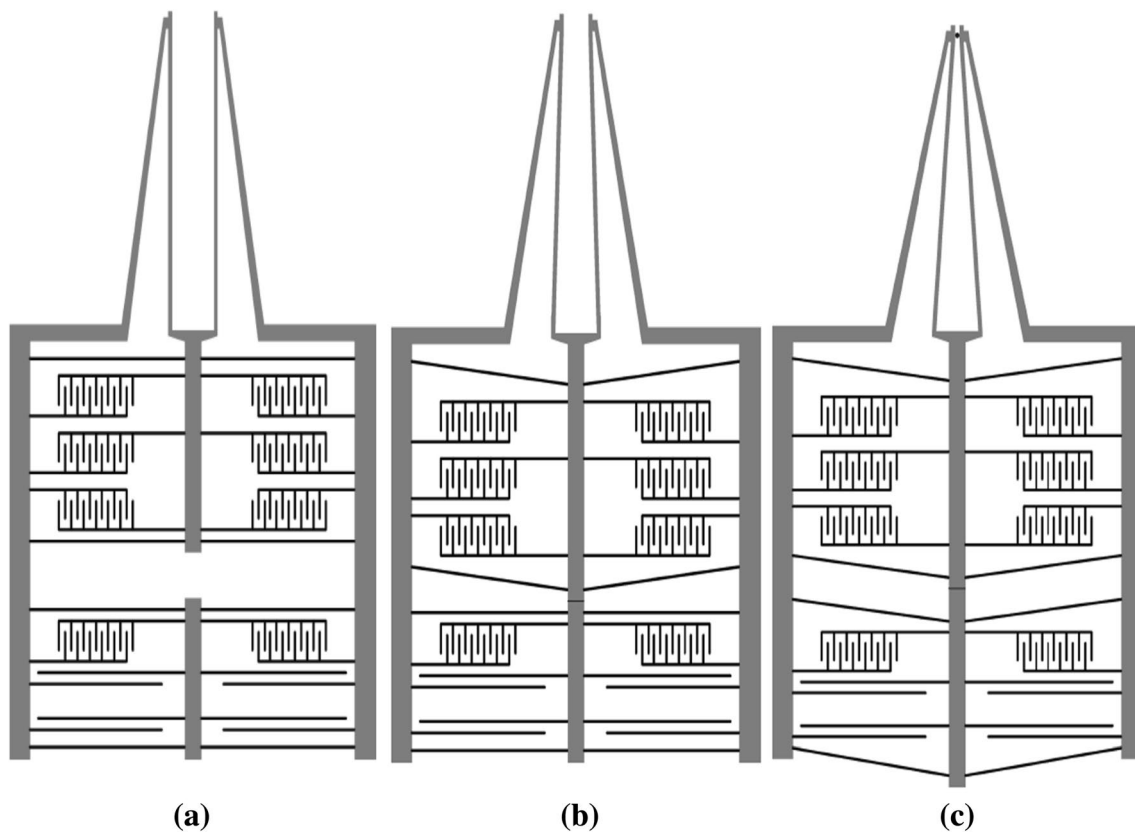
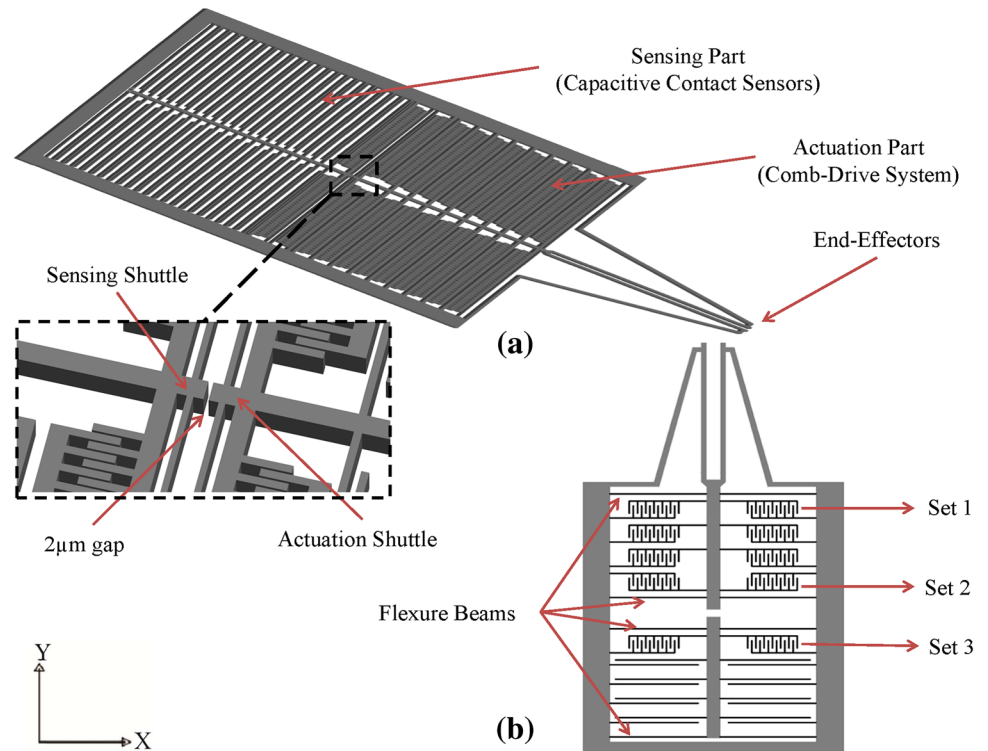


Fig. 2 Schematic diagram of the actuation process. **a** Normal position of the gripper. **b** The actuation shuttle moves to contact the sensing shuttle. Each gripper arm deflects $g_{p1} = 5 \mu\text{m}$ (no sensing

mechanism). **c** Actuation shuttle pushes the sensing shuttle $2.45 \mu\text{m}$ downward and activates the sensors. Each gripper arm deflects $g_{p2} = 6 \mu\text{m}$ at this phase

As Fig. 1 illustrates, the gripper is composed of comb drives as the actuation part, differential capacitive contact sensors as sensing part, gripper arms attached to actuation part for grasping the micro objects and flexure beams to sustain the gripper in air.

As a general description, at the first phase of actuation the DC operation voltage is applied to the comb-drive system in the actuation part. The electrostatic force attracts the actuation shuttle downward until it contacts the sensing shuttle. In this phase, the end-effectors get closer together but there is no mechanism to sense the contact between the objects and gripper arms. At the second phase of actuation, after contacting the actuation shuttle and the sensing shuttle, the DC operation voltage is increased to push the sensing shuttle downward and close the gap between the gripper arms for holding the particles. By activating the contact capacitive sensors at this phase, we are able to grip the micro object precisely and safely. After picking and transferring the particle to the desirable substrate, the DC voltage on comb-drives is removed and the shuttles are separated due to the flexure beams reaction force. Finally, by applying the electrical signals at the desired resonant frequency to specific sets of comb-drives only the actuation part and end-effectors start to vibrate whereas the sensing part will not move due to 2 μm distance between the actuation and sensing part.

Figure 2 illustrates the schematic of the actuation phase in detail. Figure 2a is the normal position of the gripper, Fig. 2b shows first actuation phase where the actuation shuttle moves downward to contact the sensing shuttle and Fig. 2c shows second actuation phase where actuation shuttle pushes the sensing shuttle and activates it for a safe grasping of the object. The dimensions of the microgripper are in Table 1.

2.1 Actuation

Lateral comb-drives are selected as the actuator. The electrostatic force required for actuation is given by Eq. 1 (Beyeler et al. 2007):

$$F_e = n\epsilon_0 \frac{tV^2}{g} \tag{1}$$

where n is total number of comb fingers, $\epsilon_0 = 8.85 \times 10^{-12}$ (C²/(Nm²)) is the permittivity of air, t is the thickness of structure, v is the operation voltage and g is the gap between the fingers. By applying the driving voltage to the stator (the comb-drives attached to the substrate) and grounding the rotor (the comb-drives attached to the actuation shuttle), the electrostatic force pushes the shuttle downward. This displacement leads to deflecting the gripper arms to close the gap and hold the object. In this work, the motion amplification of the gripper arms is 2.5, it means

Table 1 Microgripper dimensions

Gripper arm	Values
Length (μm)	1,300
Width (μm)	18
Angle with respect to vertical axis (°)	10
Gap between Arms (μm)	22
Thickness (μm)	25
Actuation part	
Total number of combs	10
Number of fingers per comb	35
Combs width (μm)	22
Finger width (μm)	8
Finger separation (μm)	2
Finger length (μm)	50
Finger overlap length (μm)	30
Distance between combs (μm)	15
Gap between shuttles	
g (μm)	2
Flexure beams	
Number of flexure beams	8
Length (μm)	800
Width (μm)	6.5
Sensing part	
Number of differential capacitive sensors	22
Width (μm)	8
d0 (μm)	10
d1 (μm)	40
Finger overlapping length (μm)	750

when the actuation shuttle moves 1 μm in y-direction, the end-effectors deflect 2.5 μm in x-direction.

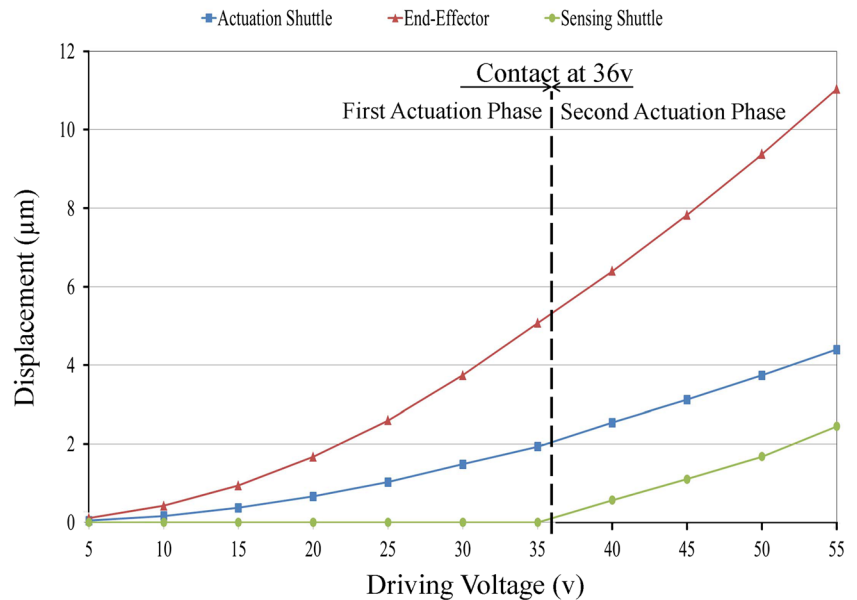
The actuation stage is divided into two phases:

1. First Actuation Phase
2. Second Actuation Phase

The objective at the first actuation phase is to close the $g = 2 \mu\text{m}$ gap between the actuation phase and the sensing shuttle. Therefore, the driving voltage (applied to the stator) is increased until the actuation shuttle contacts the sensing shuttle. FEA-based simulations are employed to estimate the voltages and the gripper behavior during the operation. Figure 3 shows displacement of the shuttles and the end-effectors over voltage as the result of the simulations. As a result, when the driving voltage is 36 V, the actuation shuttle contacts the sensing shuttle while each end-effector deflects $g_{p1} = 5 \mu\text{m}$. Note that at first actuation phase, the sensing mechanism is not activated.

After contacting the shuttles, the second actuation phase begins. The main objective of the microgripper

Fig. 3 shuttles and the end-effectors displacement over driving voltage. Contact between shuttles occurs at the driving voltage 36 V



(gripping the micro particle + contact sensing) is occurred at this Phase. Since the major goal for designing this microgripper is holding, transferring and releasing bio-particles such as living cells, the gap between the end-effectors at this phase should be compatible with the size of the target.

Voicu et al. (2007) reported that a typical dimension for a biological cell in human and multicells organisms is about 10 μm . Hence, we set the gap between the end-effectors at the second actuation phase 12 μm . Therefore, each end-effectors should travel $g_{p2} = 6 \mu\text{m}$ at this phase. In according to Fig. 3 this happens when the driving voltage is 55 V. At this voltage, the actuation shuttle pushes the sensing shuttle 2.45 μm downward and activates the capacitive contact sensors to protect the biological cells. In conclusion, each end-effector deflects $g_{p1} + g_{p2} = 11 \mu\text{m}$; $g_{p1} = 5 \mu\text{m}$ at the first actuation phase and $g_{p2} = 6 \mu\text{m}$ at second actuation phase. Figure 4a shows the total displacement of the gripper at the driving voltage 55 V. Figure 4b shows the contact between the shuttles at 55 V.

After picking and transferring the object to the desirable substrate, the driving voltage is removed from the stator combs. Principally, the flexure beams reaction force should bring back the shuttles to the normal position. However, if the adhesion force between the actuation and sensing shuttles are more than the springs force, the shuttles separation will not happen. To address this problem, we design comb-drives set2 and set3 (see Fig. 1). By applying the voltage to the stator combs of the set2 and set3, electrostatic force pushes the actuation shuttle upward, the sensing shuttle downward and results in separating the shuttles.

2.2 Sensors

Among the micro sensing mechanisms such as: piezoresistive, optical, capacitive, magnetic and piezoelectric sensors, the capacitive sensors are selected in this work as the contact sensor because of more stability, sensitivity, no hysteresis effect as well as having low power, low noise and small reactions to temperature change (Petrin 2009). Figure 5 shows the differential capacitive contact sensor mechanism which includes the desirable capacitors (C1, C2).

At the second actuation phase, when the actuation shuttle pushes the sensing shuttle downward, the sensing shuttle movement increases the gap between the capacitors plates at one side and decreases the gap on the other side proportionally. In other words, capacitance increases on one side and decreases on the other side. The changes can be measured by a capacitance readout chip such as MS3110 which is able to generate output voltage proportional to the capacitance change (Bazaz et al. 2011). When the end-effectors deflect to grasp the target, the change in capacitance continues. Gripping the micro object causes that the end-effectors do not move further which leads to no capacitance change. Consequently, the differential contact capacitive sensor recognizes the contact between the object and the end-effectors and avoid exerting excessive force to the target.

C1 and C2 capacitances are defined by (Bazaz et al. 2011):

$$C1 = n\epsilon_0 \frac{A}{d_0 + y} + C_{fringe} \quad (2)$$

$$C2 = n\epsilon_0 \frac{A}{d_0 - y} + C_{fringe} \quad (3)$$

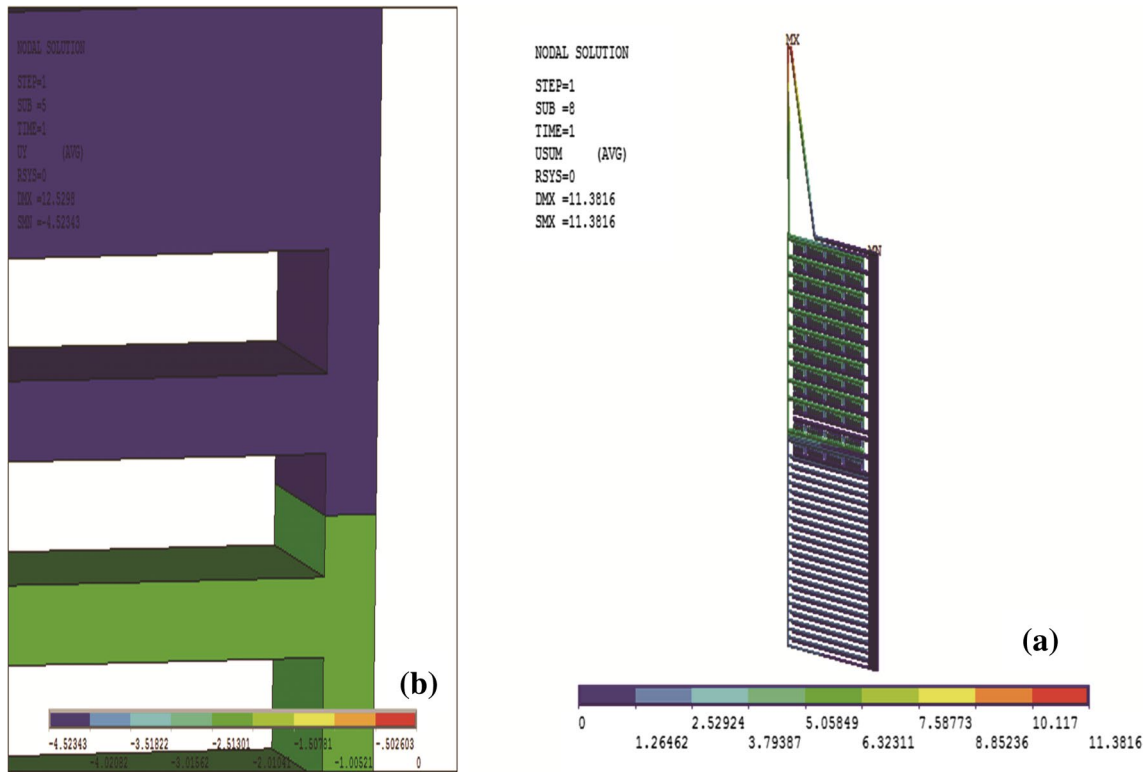


Fig. 4 **a** Total displacement of the microgripper at the driving voltage 55 V. **b** Contact between the shuttles at 55 V (the values show displacement of the shuttles in y-direction)

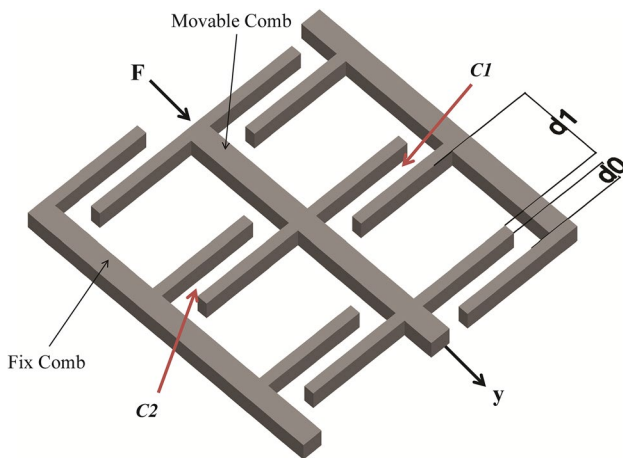


Fig. 5 Schematic drawing of a differential capacitive sensor

where n is the number of capacitance, $\epsilon_0 = 8.85 \times 10^{-12} \text{ (C}^2/\text{Nm}^2\text{)}$ is the permittivity of air, A is overlap area between two plates, d_0 is the initial gap between the plates, y is the displacement of the sensing shuttle at second actuation phase and C_{fringe} is capacitance produced due to fringe fields.

Figure 6 shows air elements (red elements) in FEA simulation for one pair of capacitors (the elements of solid

parts; fixed and movable parts are not shown). $C1$ and $C2$ are the capacitors which are increased and decreased by moving the sensing shuttle downward respectively. To calculate the values of $C1$ and $C2$ by FEA simulation, the boundary conditions are applied to the nodes of these elements. Therefore, the mutual nodes of air elements and fixed parts and plates are fixed and stimulated by voltage and on the other hand, the mutual nodes of air and sensing shuttle and moving plates are grounded ($V = 0$). The simulations are carried out for one pair of capacitors and then the results are multiplied by the number of capacitors to get the total values. By recording these values and calculating the total capacitors theoretically (Eqs. 2, 3), Fig. 7 is obtained. In Fig. 7, $CS1$ and $CS2$ show the results of simulations for the total capacitors on both sides of the sensing shuttle and $CT1$ and $CT2$ are the theoretical results of the total capacitors. However the reason for the 0.093 pF difference between the results is parasitic capacitance which is not included in the theoretical modeling.

2.3 Releasing

Structural vibration is the most frequent problem which threatens the precise gripping and releasing process (Park and moon 2005). The vibration of the microgripper's

Fig. 6 FEA model of one differential capacitive sensor. Red elements indicate air gap between the plates

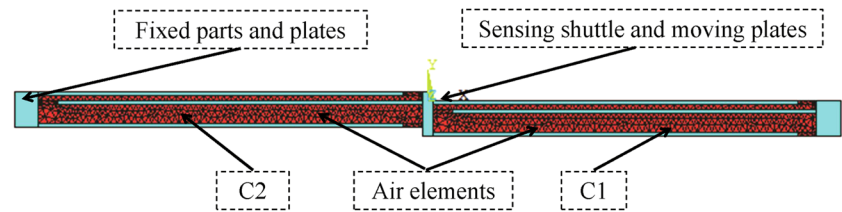
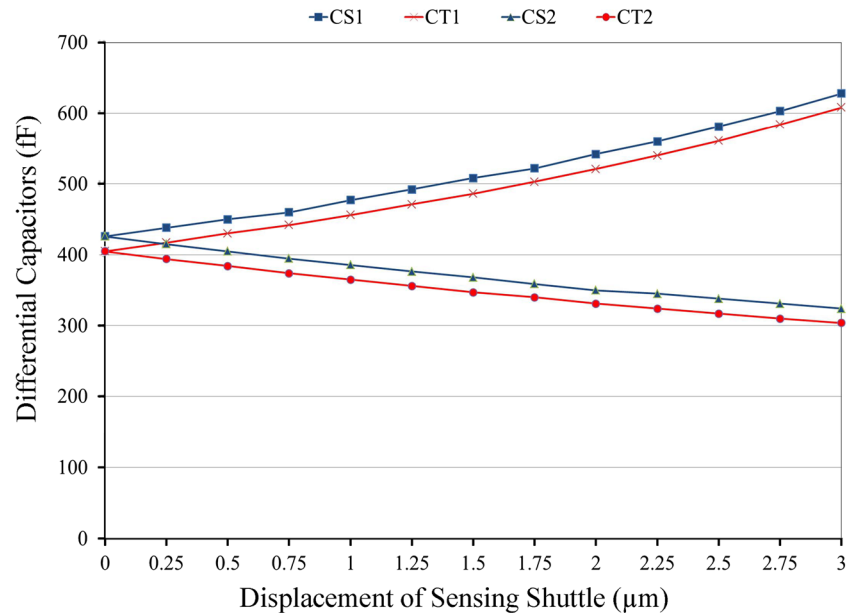


Fig. 7 Total values of differential capacitive sensors versus displacement of the sensing shuttle. *CS1*, *CS2* are simulation results; *CT1*, *CT2* are theoretical results



support (or manipulator; a table on which the microgripper is mounted) can cause large positioning errors which even makes it impossible to grip objects or can excite a resonance in the grippers and results in loss of the grabbed object (Park and moon 2005; Molhave 2004). To block structural vibrations the microgrippers manipulator (support) should be highly stiff with high fundamental natural frequencies (Park and moon 2005).

Park and moon (2005) calculated the fundamental resonant frequency of the gripper's fingertips (191 Hz) and designed the support with high resonant frequency (600 Hz) to protect the device from structural vibration. Bazaz et al. (2011) and Chen et al. (2010a, b) investigated the first modes of the gripper vibration by FEA simulation (see Table 2) before testing the gripper to avoid vibration of the gripper support at these frequencies in testing procedure. In order to find these values for this work, we use FEA Modal analysis. Table 2 shows the results of the modal simulations.

The first resonant frequency (3.07 kHz) is related to the sensor part which vibrates in-planly. Due to 2 μm gap between the shuttles, this vibration does not have effect on the end-effectors. The second one (4.83 kHz) is the resonant frequency of the actuation part which vibrates in-planly. Figure 8 shows the displacement of the actuation part of the gripper at the resonant frequency (4.83 kHz).

At the release stage, the free end of object is placed on the substrate, if the adhesion between object and substrate is larger than the adhesion between object and gripper surface, it will be released. Otherwise, by vibrating the end-effector, the adhesion force between particle and gripper's arm decreases due to inertial effects (Chen et al. 2010a, b).

In order to overbalance the adhesion force between the micro object and the end-effector and facilitate the release process, we apply the electrical signals to the combs of set1 and set2 (see Fig. 1) to generate vibration at the end-effectors in-planly. Since the electrostatic vibration of the

Table 2 Microgrippers resonant frequencies

Modes	1	2	3	4	5	6
Bazaz et al. (2011)	4.522	5.488	8.187	8.624	11.918	14.228
Chen et al. (2010a, b)	4.2384	5.3758	7.8717	10.081		
This work	3.07	4.83	6.81	9.35	15.2	18.8

All values are in kHz

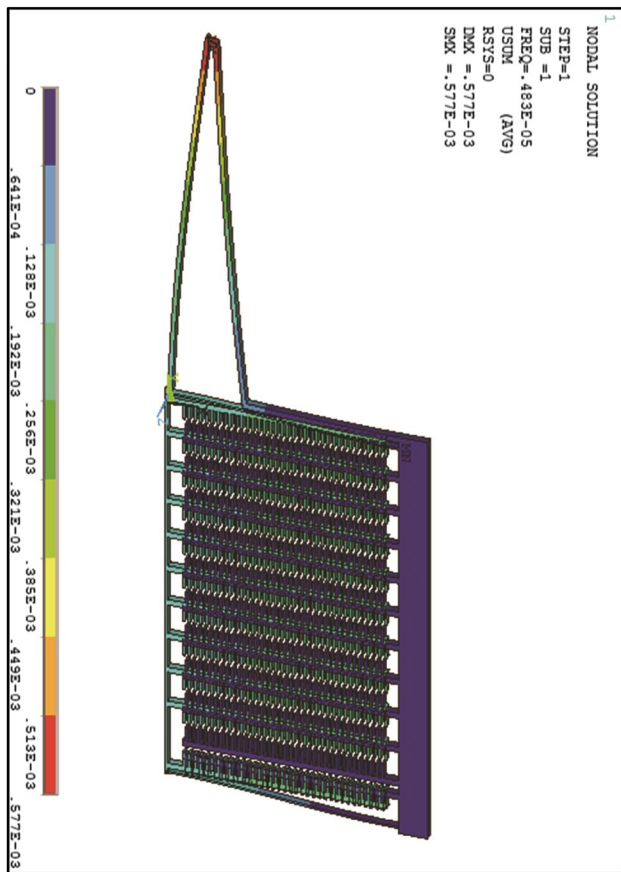


Fig. 8 Modal FEA simulation result for the actuation part of the microgripper at the resonant frequency (4.83 kHz)

microgripper at the release phase is in-planely, we apply the electrical signals with the frequency equal to the second resonant frequency of the gripper $F_r = 4.8$ kHz [at which the actuation part vibrates in-planely (see Fig. 8)] to the combs of set1 and set2. Figure 9 shows the two pulse signals that is applied to the stators of set1 and set2 for generating vibration ($T_s = 1/F_r$). Practically, by sweeping the frequency of these signals around the desired resonant frequency, vibration at the end effectors is generated.

Since the actuation part vibrates in-planely, the sliding damping between the comb fingers plays an important role. Table 3 shows damping parameters briefly.

Sliding damping factor is given by Acar and Shkel (2009):

$$c_{slide} = \mu_{eff} \frac{A}{d} \tag{4}$$

where A is overlap area between the comb fingers, d is gap between the comb fingers and μ_{eff} is effective coefficient of air viscosity. The effective viscosity is given by Acar and Shkel (2009):

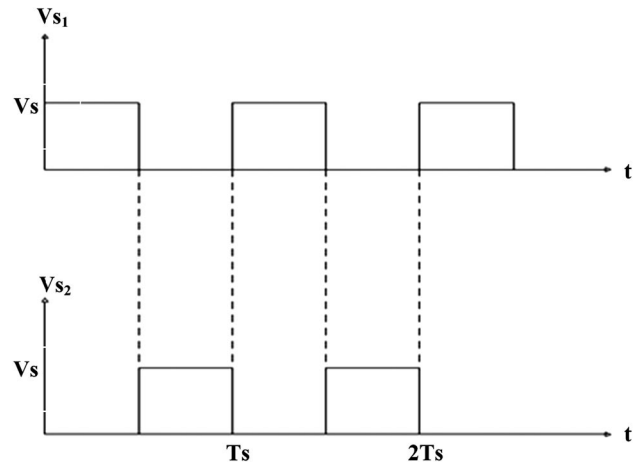


Fig. 9 Pulse signals that applied to the stators of set1 and set2

Table 3 Damping parameters

Parameter	Value	Descriptions
μ (MPa-s)	1.86×10^{-11a}	Air viscosity
λ (μm)	6.7×10^{-2a}	Gas (air) mean free path
d (μm)	2	Gap between comb fingers
C_{slidef}	0.1×10^{-4}	Sliding damping factor of the comb drive fingers

^a Riaz et al. (2011)

$$\mu_{eff} = \frac{\mu}{1 + 2K_n + 0.2K_n^{0.788} e^{-\frac{K_n}{10}}} \tag{5}$$

K_n is Knudsen number which is calculated by Acar and Shkel (2009):

$$K_n = \frac{\lambda}{d} \tag{6}$$

where λ is gas (air) mean free path.

To illustrate this subject, Harmonic FEA simulation is employed to estimate the end-effectors vibration amplitude at the resonant frequency. Figure 10 shows vibration amplitude of the end effectors versus frequency. The end-effector vibration amplitude is 628 nm whereas the amplitude of the electrical signals ($vs1, vs2$) is set 20 V.

3 Proposed fabrication process

A silicon-on-insulator (SOI) wafer with a device layer of $25 \mu\text{m}$ is proposed to be used for fabricating the microgripper. Figure 11 illustrates the fabrication sequence based on (Beyeler et al. 2007):

Fig. 10 Vibration amplitude of the end-effector versus frequency

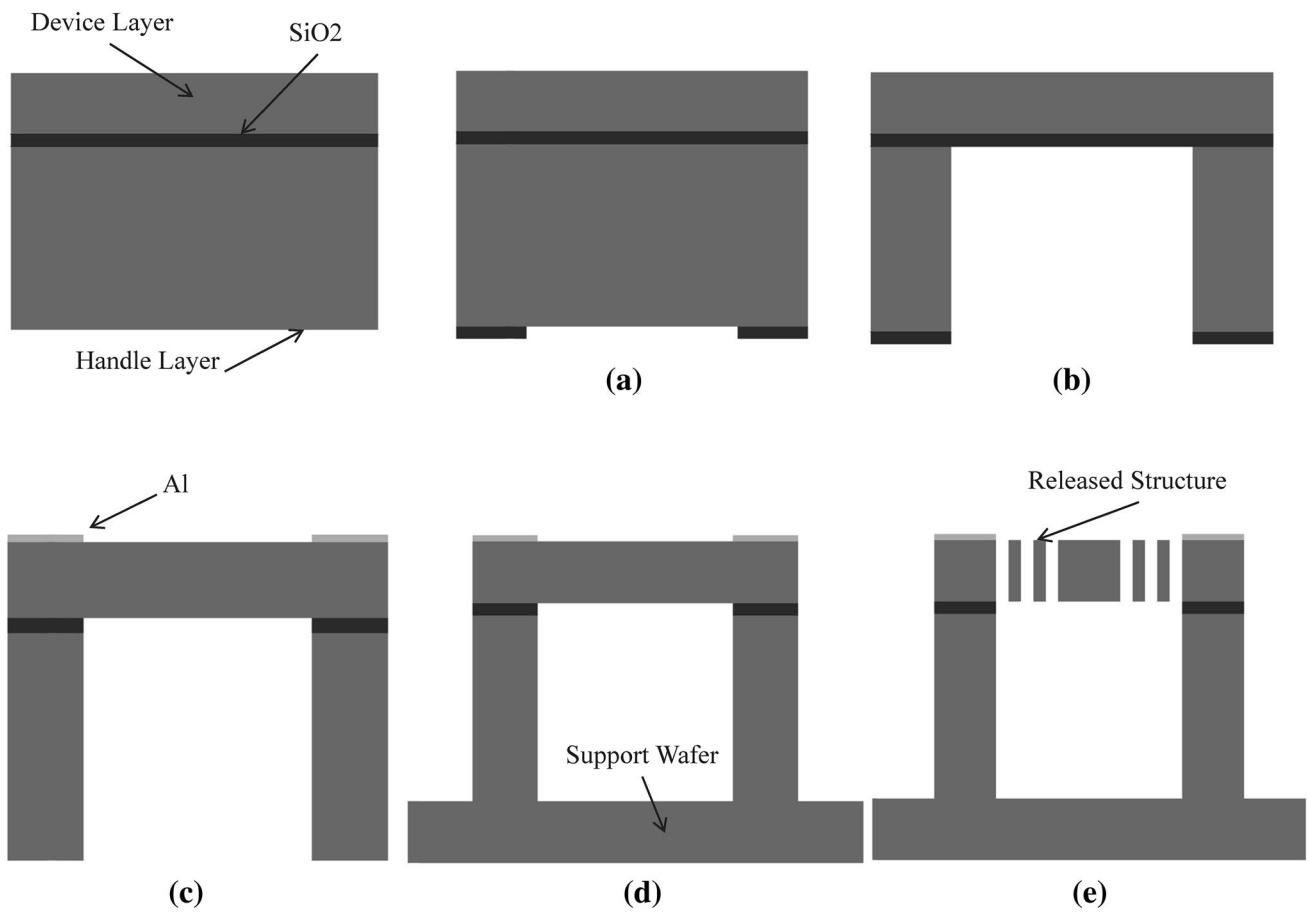
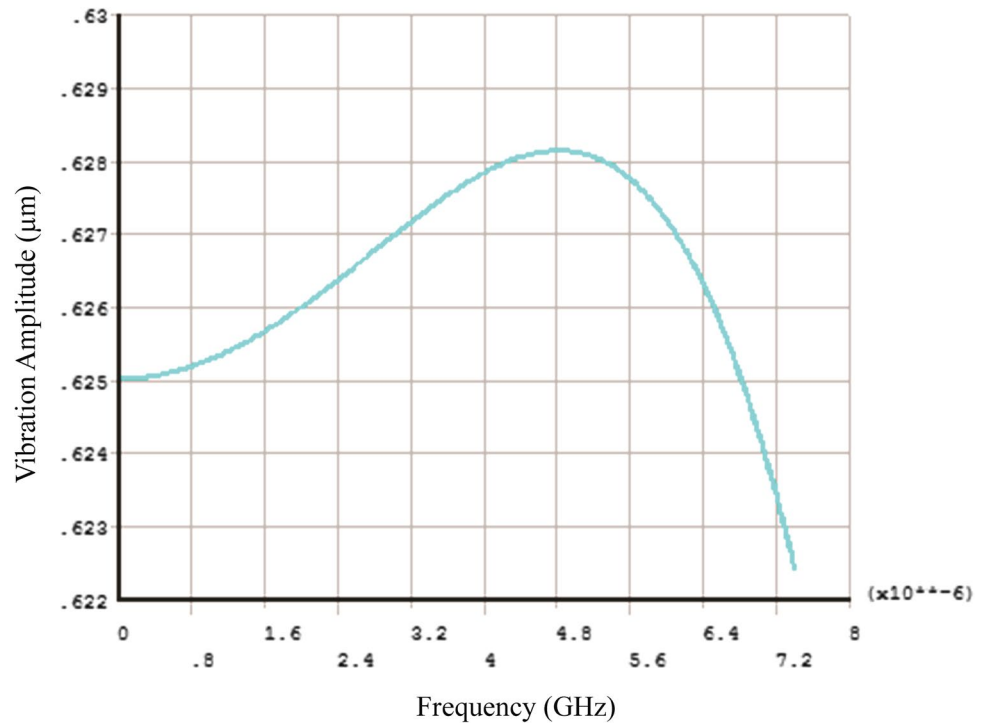


Fig. 11 Proposed fabrication process

- (a) Silicon oxide layer (SiO₂) is deposited on the backside of the wafer and patterned using reactive ion etching (RIE).
- (b) The backside silicon is etched using deep reactive ion etching (DRIE). The buried SiO₂ acts as an etch stop.
- (c) The buried SiO₂ is etched using RIE. A thin layer of Al is evaporated and patterned to form electrodes on the device layer.
- (d) The SOI wafer is bond to a support wafer using heat conductive grease.
- (e) The device layer, including the flexures, comb-drives, and gripper arms, is etched using DRIE dry etching to form the designed microgripper.

4 Conclusion

In this study, we reported a novel electrostatically actuated microgripper integrated with capacitive contact sensor to protect the bio cells from damaging. Moreover, at the release phase the gripper is able to vibrate the end-effectors in-plane to overcome the adhesion forces by inertial effects. The 2 μm gap between the actuation part and sensing part causes that the capacitors do not participate at vibration stage. At the actuation phase, the gap between the shuttles is closed at the driving voltage 36 V. Afterward, the gripper is able to grasp the object (living cells) at the size of 12 μm at the driving voltage 55 V while the capacitive contact sensors are active. At the release phase, the operation voltage is removed and the shuttles bring back to the normal position by the springs reaction force and the electrostatic force (comb drive set2 and set3). By applying the electrical signals at the desired resonant frequency (4.83 kHz) to the comb-drive set1 and set2, electrostatically in-plane vibration is generated to overbalance the adhesion force and facilitate the release process.

References

- Acar C, Shkel A (2009) MEMS vibratory gyroscopes: structural approaches to improve robustness. Springer, New York
- Arai F, Andou D, Fukuda T (1996) Adhesion forces reduction for micro manipulation based on micro physics. In: Paper presented at the IEEE conference, San Diego, 1996
- Bazaz SA, Khan F, Shakoor RI (2011) Design, simulation and testing of electrostatic SOI MUMPs based microgripper integrated with capacitive contact sensor. *Sens Actuators A Phys* 167:44–53
- Beyeler F, Neild A, Oberti S, Bell DJ, Sun Y, Dual J, Nelson BJ (2007) Monolithically fabricated microgripper with integrated force sensor for manipulating microobjects and biological cells aligned in an ultrasonic field. *J Microelectromech Syst* 16:7–15
- Chen BK, Zhang Y, Sun Y (2009) Active release of microobjects using a MEMS microgripper to overcome adhesion forces. *J Microelectromech Syst* 18:652–659
- Chen T, Chen L, Sun L, Rong W, Yang Q (2010a) Micro manipulation based on adhesion control with compound vibration. In: Paper presented at the International Conference on Intelligent Robots and Systems, Taipei, Taiwan, October 18–22, 2010
- Chen T, Sun L, Chen L, Rong W, Li X (2010b) A hybrid-type electrostatically driven microgripper with an integrated vacuum tool. *Sens Actuators A Phys* 158:320–327
- Chronis N, Lee LP (2005) Electrothermally activated SU-8 microgripper for single cell manipulation in solution. *J Microelectromech Syst* 14:857–863
- Demaghsi H, Mirzajani H, Ghavifekr HB (2013) Design and simulation of a novel metallic microgripper using vibration to release nano objects actively. *J Microsyst Technol*. doi:10.1007/s00542-013-1888-7
- Duc TC, Lau GK, Creemer JF, Sarro PM (2008) Electrothermal microgripper with large jaw displacement and integrated force sensors. *J Microelectromech Syst* 17:1546–1555
- Fang Y, Tan X (2006) A dynamic JKR model with application to vibrational release in micromanipulation. Paper presented at the Intelligent Robots and Systems Beijing, 9–15 Oct 2006
- Fuchiwaki O, Ito A, Misaki D, Aoyama H (2008) Multi-axial micro-manipulation organized by versatile micro robots and micro tweezers. In: Paper presented at IEEE International Conference on Robotics and Automation, ICRA 2008, Pasadena, CA, USA
- Goldfarb M, Celanovic N (1999) A flexure-based gripper for small-scale manipulation. *Robotica* 17:181–187
- Kim CJ, Pisano AP, Muller RS, Lim MG (1992) Polysilicon microgripper. *Sens Actuators A Phys* 33:221–227
- Kim K, Nilsen E, Huang T, Kim A, Ellis M, Skidmore G, Lee JB (2004) Metallic microgripper with SU-8 adaptor as end-effectors for heterogeneous micro/nano assembly applications. *Microsyst Technol* 10:689–693. doi:10.1007/s00542-004-0367-6
- Kohl M, Krevet B, Just E (2002) SMA microgripper system. *Sens Actuators A Phys* 97:646–652
- Kyung JH, Ko BG, Ha YH, Chung GJ (2008) Design of a microgripper for micromanipulation of microcomponents using SMA wires and flexible hinges. *Sens Actuators A Phys* 141:144–150
- Mackay RE, Le HR, Clark S, Williams JA (2013) Polymer microgrippers with an integrated force sensor for biological manipulation. *J Micromech Microeng* 23:015005
- Millet O, Bernardoni P, Régnier S, Bidaud P, Tsitsiris E, Collard D, Buchaillot L (2004) Electrostatic actuated micro gripper using an amplification mechanism. *Sens Actuators A Phys* 114:371–378
- Molhave K (2004) Tools for in-situ manipulation and characterization of nanostructures. Dissertation, MIC-Department of Micro and Nanotechnology Technical University of Denmark
- Park J, Moon W (2005) The systematic design and fabrication of a three-chopstick microgripper. *Int J Adv Manuf Technol* 26:251–261
- Petrin AA (2009) Processing of sensor information in micro and nano manipulation. *Automat Doc Math Ling* 43:355–362
- Raghavendra MRA, Kumar AS, Jagdish BN (2010) Design and analysis of flexure-hinge parameter in microgripper. *Int J Adv Manuf Technol* 49:1185–1193. doi:10.1007/s00170-009-2478-9
- Riaz K, Bazaz SA, Saleem MM, Shakoor RI (2011) Design, damping estimation and experimental characterization of decoupled 3-DoF robust MEMS gyroscope. *Sens Actuators A Phys* 172:523–532
- Sinan Haliyo D, Régnier S, Bidaud P (2003) Manipulation of micro-objects using adhesion forces and dynamical effects. *J Exp Robotics VIII* 382–391
- Stavrov V, Tomerov E, Hardalov C et al (2010) Low voltage thermomechanically driven monolithic microgripper with piezoresistive feedback. In: Ratchev S (ed) *Precision Assembly Technologies and Systems*. Springer, New York
- Tang WC, Nguyen TCH, Howe RT (1989) Laterally driven polysilicon resonant microstructures. *Sens Actuator* 20:25–32

- Varona J, Saenz E, Fiscal-Woodhouse S, Hamoui AA (2009) Design and fabrication of a novel microgripper based on electrostatic actuation. In: Paper presented at IEEE International Midwest Symposium on Circuits and Systems (MWSCAS'09). 827–832
- Voicu R, Esinenco D, Müller R, Eftime L, Tibeica C (2007) Method for overcoming the unwanted displacements of an electro-thermally actuated microgripper. *J Young* 1
- Volland BE, Heerlein H, Rangelow IW (2002) Electrostatically driven microgripper. *Microelectron Eng* 61:1015–1023
- Volland BE, Ivanova K, Ivanov T et al (2007) Duo-action electro thermal micro gripper. *Microelectron Eng* 84:1329–1332